Comparative Study of Electron Temperature and Ion Energy in Two Different Magnetic Nozzle Thruster Designs

IEPC-2024-154

Presented at the 38th International Electric Propulsion Conference, Toulouse, France
June 23-28, 2024

Clara E. Schäfer*, Jens Schmidt†, Felix Plettenberg‡, Yung-An Chan§, Martin Grabe¶, Jan Martinez-Schramm‖
German Aerospace Center, 37073 Göttingen, Germany

and

Kristof Holste**, and Peter J. Klar††
Justus Liebig University, 35392 Giessen, Germany

I. Abstract

Conventional ion thruster technologies face challenges such as electrode and grid erosion and the need for additional neutralizer devices. In this article, we discuss two thruster concepts that achieve plasma acceleration by means of a magnetic nozzle, and thus avoid the need of a neutralizer device. The concept of a magnetic nozzle converting the thermal energy available in the electrons to ion kinetic energy is a well accepted model in the community. We discuss a thruster concept based on electrode-less electron cyclotron resonance plasma generation via a slot antenna design. The geometry of this thruster concept results in a converging-diverging character of the magnetic field topology along the plume direction. To this date it is not known in which way this electrode-less coupling of the microwave influences the electron dynamics and thus the ion energy. To understand the correlation between ion energy and electron temperature of this thruster system, it is compared with a well-known thruster prototype operating on similar principles, however, realizing microwave coupling in a different way. Both thruster designs operate within comparable power, frequency, and volume flow ranges. Maximum ion energy is measured for both thrusters using a retarding potential analyzer under the same surrounding conditions. Additionally, the electron temperature is measured with a Langmuir probe for various operation points, such as variable input power, volume flow, set frequency, and argon and xenon as propellant.

II. Introduction

Electrodeless plasma thrusters with magnetic nozzles (MN) offer high operational flexibility and longer lifetimes. They are of great interest for long-distance space travel and become prominent in recent thruster development.[1] Resembling the traditional "de Laval" nozzle, a MN typically possesses a divergent magnetic

*PhD student, Spacecraft Department, clara.schaefer@dlr.de.
†Research Associate, Spacecraft Department, jens.schmidt@dlr.de.
‡Student, Spacecraft Department, felix.plettenberg@dlr.de.
§Research Associate, Spacecraft Department, yung-an.chan@dlr.de.
¶Head of Rarefied Flows Group, Spacecraft Department, martin.grabe@dlr.de.
‖Head of Spacecraft Department, jan.martinez@dlr.de.
**Laboratory Head of Ion Thruster Research Group, Institute of Experimental Physics I, kristof.holste@physik.uni-giessen.de.
††Head of Ion Thruster Research Group, Institute of Experimental Physics I, peter.j.klar@physik.uni-giessen.de.

field structure caused either by an applied or a self induced magnetic field. The divergent field guides and accelerates a magnetized plasma jet into vacuum.[2] The diverging magnetic field radially confines the plasma and helps the conversion of perpendicular into parallel plasma motion. The electrostatic field converts the thermal energy motion of the electrons into ion kinetic energy. Therefore the electron dynamics plays a crucial role in configuring the electrostatic field in the plume, responsible for ion acceleration and ultimately thrust generation.[1] One advantage of this approach to plasma acceleration is the absence of a direct contact between the plasma and the structure walls. This reduces wall losses and simplifies plasma description. Moreover, no electrodes are required for plasma acceleration or neutralization. Instead, the MN utilizes the expanding electron gas to neutralize the ion beam without the need for additional cathode installation.[1] This extends the thruster's lifetime and eliminates the need for complex neutralizer devices. Additionally, the capability to use various propellants is advantageous, along with the scalability and adaptability of a MN.[2] Various thrusters, both established and under development, exhibit different characteristics from the perspective of plasma generation and heating, yet they all realize the physics of quasi-neutral, quasi-collisionless plasma expansion in a MN.[1]

In the following, we discuss the thruster concept DEEVA (*DLR Electrodeless ECR Via microwave plasma Accelerator*), which allows electrode-less plasma generation by microwaves, fulfilling the electron cyclotron resonance (ECR) condition.[3] Plasma acceleration is achieved by the converging-diverging magnetic field of a MN. This thruster concept is compared with a prototype of the well-known thruster concept developed by the Office national d'études et de recherches aérospatiales under the project *Magnetic Nozzle Electron Cyclotron Resonance Thruster* (MINOTOR).[4–8] While both thruster concepts employ a MN, are of similar size, and are designed to operate within a similar frequency and power range, they differ in terms of the approach for microwave coupling into the plasma. This results in different magnetic field topology requirements as well. The microwave coupling in case of MINOTOR is achieved by a coaxial coupling structure, where the inner conductor is directly exposed to the plasma. The DEEVA thruster concept uses an electrode-less coupling by an annular waveguide (ring cavity) defined by two resonant coupling slots into the plasma discharge chamber made of quartz. The idea of using such a slot antenna (SLAN) for a thruster is based on the work by Korcez et al.[9]
In recent years, several studies have explored the connection between electron temperature and ion energy, and have addressed the effect of electron cooling on ion energy by making use of the polytropic expansion law.[1,10–12] As it is reported in literature, a constant ratio value of electron temperature and maximum ion energy, describing the polytropic index, was determined. The resulting ratios were described in dependence on magnetic field strength. Experimental findings have shown relatively stable ratios of electron temperature to ion energy across a wide range of parameters. However, while polytropic models offer simplicity and approximate the effects of electron cooling, their accuracy in describing plasma expansion processes has been questioned by theoretical studies.[11,12]

A comprehensive understanding of the relationship between electron dynamics and heat flux/ion energy in expanding plasma systems remains elusive for the relatively new DEEVA thruster. Investigating the effect of changing operational parameters—such as varying input power, frequency settings, and volume flow of propellant—on the correlation between electron temperature and ion energy is essential. Comparing the DEEVA and the MINOTOR prototype under the same operating conditions (e.g. same vacuum chamber, similar background pressures, same diagnostic tools) allows us to carry out detailed studies of the impact of the microwave coupling method and magnetic field topology on plasma parameters. In particularly we vary the operation conditions of the thrusters and conduct retarding potential analyzer (RPA) as well as Langmuir probe (LP) measurements for a determination of electron temperature and ion energy. Preliminary studies showed that the determined electron temperatures and ion energies in case of the DEEVA thruster are higher, when performing with argon as propellant instead of xenon. Therefore, the discussed operational changes in the following comprises varying propellant (xenon and argon), varying input power, changing frequency set and variable volume flow.

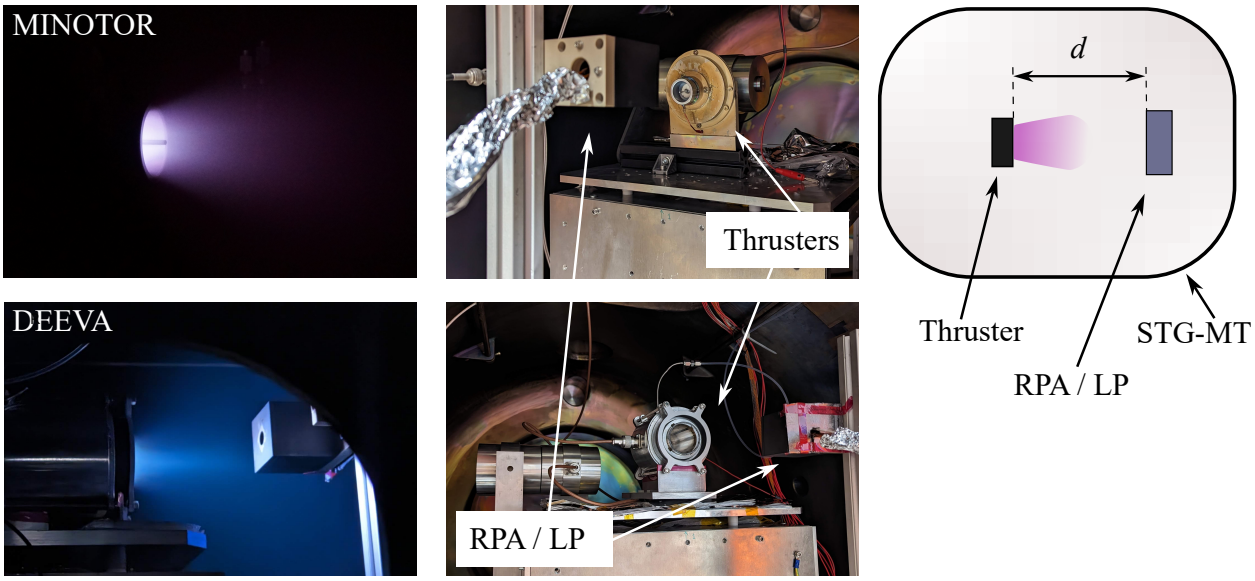

Figure 1. Test set up of the MINOTOR and DEEVA prototype and diagnostics in the vacuum chamber STG-MT. On the top row, one can see MINOTOR, on the bottom the DEEVA prototype is pictured. The left column shows the running thrusters and their beams, the right column depicts the test set up, with the thrusters, as well as the diagnostic tools, the retarding potential analyzer (RPA) and the Langmuir probe (LP). On the right hand side, one can see the top view of the test set up. With the thruster on the left and the diagnostics in a distance $d = 100\,\mathrm{mm}$ from the thrusters exit plane.

III. Methods and experimental set up

A. Test facility and set up

The experiments are conducted at the DLR in Göttingen in the vacuum facility *Simulationsanlage für Treibstrahlen Göttingen - Miniatur Triebwerke* (STG-MT). The chamber has a length of 1 m and a diameter of 1.1 m. It is equipped with two backing pumps, a rotary vane pump and a roots pump yielding a base pressure of 10^{-3} mbar. For lower pressure ranges a turbomolecular pump is added allowing pressure ranges of 10^{-6} mbar and background pressures during thruster operation in the range of 10^{-5} mbar. For the operation of the thrusters, we use the microwave signal generator KU-SG 2.45-250A of the company Kuhne elecronics Gmbh as well as the Bronkhorst mass control unit (MCU) for maximum 50 sccm air. It has to be mentioned that in the following we use the term 'input power' to describe the power emitted by the microwave generator. For upcoming experiments, a bi-directional coupler or a vector network analyzer will be used to determine the power depleted in the plasma. Therefore, with the term 'input power' we refer to the forward sent power, with a given uncertainty to what degree the forward sent power is actually coupled into the plasma. The gases in use are xenon and argon. The mapping of each thruster is performed as follows: For all operation points the plasma is measured with LP in $d = 100 \pm 0.5\,\mathrm{cm}$ distance to the thruster exit. The ion energy is investigated by means of RPA measurements. Multiple measurements at the same thruster setting are performed and yield the experimental uncertainty of the results. The set up can be seen in Figure 1.

B. Thrusters under investigation

The operating principle of both the ECR thrusters with MN is the ionization of the propellant via ECR and the acceleration by a divergent magnetic field.[5,13,14] A schematic of the thrusters can be seen in figure 2. In presence of a magnetic field, charged particles (electrons and ions) are trapped along the magnetic field lines in such a way that they are circulating (gyrating) around the field lines, due to Lorentz forces.[14] Since electrons are much lighter than ions, their movement about the magnetic field lines is decisive for the behaviour of a magnetized plasma.[14] Additionally to the gyration about the field lines, a drift motion is superimposed, if a velocity component parallel to the magnetic field lines is present.[13,14] The angular frequency of the electrons around the field lines is given by the cyclotron frequency. If an electromagnetic wave with that cyclotron frequency is applied, the electron is resonantly accelerated by the electric field of

the wave. It absorbs the energy of the electromagnetic wave, gains kinetic energy and increases the impact ionization process rate.[13,14] Given the magnetic field of 87.5 mT, one comes to a microwave frequency of 2.45 GHz for resonant excitation.

The acceleration of the produced ions is assumed to originate from two processes: First, the faster reaction of the electrons to density disturbances or density gradients, due to their lower mass.[14,15] The pressure gradient between the thruster interior and the environment leads to the faster response of electrons in comparison to the heavier ions.[14] As a result of the charge separation an ambipolar field forms, leading to the acceleration of the ions towards the negative space charge.[14] The second driving mechanism is the gradient in the magnetic field. Due to the inhomogenity of the magnetic field parallel to the magnetic field lines, the magnetic moment μ of the charged particles (forming due to the gyration of the particles about the magnetic field lines) and the mass of the particle m, can be used to formulate an acceleration ($\dot{v}_{||}$) opposite to the gradient direction $\nabla_{||}B$:[14,16]

$$m\dot{v}_{||} = -\mu\nabla_{||}B. \tag{1}$$

This force can cause particles to reflect in the converging sections of a MN. This phenomenon, known as the magnetic mirror effect, has been the subject of investigation in several recent studies aimed at modeling MN behavior.[1,2,12,17] Depending on the magnetic field ratio (the ratio of maximum field strength to minimum field strength, $\frac{B_0}{B_{\max}}$), a critical pitch angle α leading to particle reflection can be determined:[14]

$$\sin\alpha > \sqrt{\frac{B_0}{B_{\max}}}. \tag{2}$$

The pitch angle is defined by the parallel and orthogonal velocity components of the particle ($\tan\alpha = \frac{v_\perp}{v_{||}}$). Thus, in a convergent–divergent MN, the axial motion of individual ions or electrons is governed by both electrostatic and magnetic mirror forces.[1] While the electrostatic field accelerates ions and decelerates electrons axially in the convergent and divergent MN regions, the magnetic mirror force decelerates both ions and electrons in the convergent part and accelerates them axially in the divergent part.
As reported in Lafleur et al.,[10] stronger magnetic fields result in smaller ion energy to temperature ratios, according to a non-Maxwellian kinetic model and Faraday probe measurements. Additionally, it was concluded that the magnetic field does not cause additional ion acceleration in the downstream region of the nozzle, as evidenced by the fact that ion energy values will remain high even if the magnetic field is turned off.[10] In these studies, the ratio of electron temperature to maximum ion energy often exhibited a rather constant value. Specifically, in the absence of a magnetic nozzle, a ratio of 7 was observed, while stronger magnetic fields led to a ratio of about 4. Ion energies were measured in the range of 150 eV, with electron temperatures exceeding 20 eV.[10] However, it is important to note that while the ECR thruster design studied by Lafleur et al. bears resemblance to the MINOTOR prototype examined in our study, the entire thruster setup has undergone changes during the development, regarding geometry and performance. For example, in the previous study, the magnetic field was generated by coils, allowing a control of magnetic field strength, while the MINOTOR prototype in our case is equipped with permanent magnets.

C. Langmuir probe evaluation

One of the most technically simple, yet difficult to interpret, diagnostics tools is the Langmuir probe (LP).[14] This probe consists of one, two or three conductive electrodes of various shapes, directly brought into the plasma. If a single electrode probe is introduced into the plasma and the voltage U is varied with respect to a reference potential. The current-voltage characteristic obtained, can be divided into three ranges according to Demidov et al.:[18] For sufficiently negative probe voltage the probe collects mainly positive ions. In the transition part of the characteristic the probe collects ions and electrons.[18] If no current is measured, the ion and electron currents are equal, this is the floating potential Φ_{fl}.[18] For the set voltage equal to the plasma potential Φ_{P} the characteristic may show a kink ('knee') because the potential changes character from attracting ions and repelling electrons to repelling ions and attracting electrons.[18] For higher positive voltages the probe only collects electrons.[18] By measuring this current-voltage characteristic it is possible to capture properties of the plasma, such as temperatures, potentials, densities etc.[14] The exctraction of these plasma parameters requires an appropriate theory. We apply the Druyvestein method for the single Langmuir probe measurement.[19,20] Using that we determine directly the EEDF ($f(E)$) based on the second

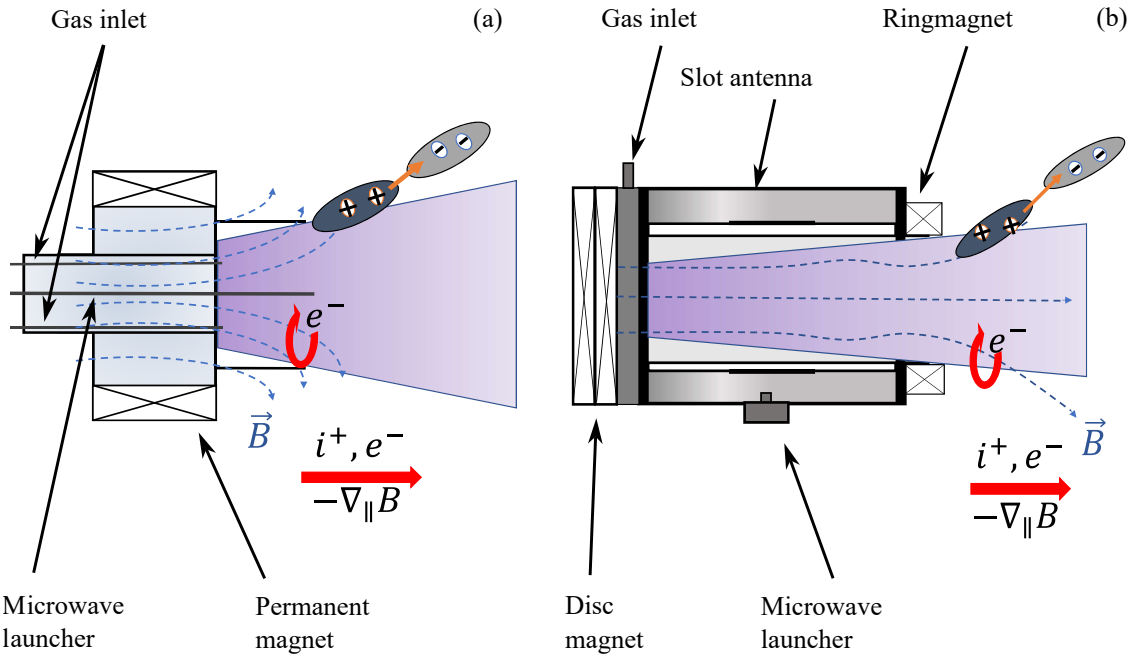

Figure 2. Schemes of the ECR thrusters. MINOTOR is pictured on the left, the thruster is pictured in black. The magnetic field lines are pictured in blue, and the particle motions are pictured in red. e^- are the electrons and i^+ are the ions. As for DEEVA on the right: The slotted antenna (consisting of two cylinders and the slots), the quartz tube and the gas inlet is indicated. Here the magnetic field lines are also pictured in blue, and the particle motions are pictured in red. For both thrusters the ambipolar electric field is indicated in orange. Additionally for both thrusters the microwave launchers are depicted.

derivative of the measured current voltage characteristic $\frac{\mathrm{d}^2 I_e}{\mathrm{d}U^2}$, the probe surface A_P, the electron mass m_e and charge e and the energy E of the electron hitting the probe:

$$f(E) = \frac{2}{e^2 A_\mathrm{P}} \sqrt{2 m_\mathrm{e} E} \frac{\mathrm{d}^2 I_e}{\mathrm{d}E^2}. \tag{3}$$

It should be noted that here we correct the measured current I_0 by subtracting the ion current I_i to get the second derivative of the electron current $I_\mathrm{e} = I_0 - I_\mathrm{i}$. By taking the moment of the distribution function we obtain the electron temperature T_e of the plasma:

$$T_\mathrm{e} = \frac{2}{3 n_\mathrm{e}} \int_0^\infty f(E)\, E \,\mathrm{d}E. \tag{4}$$

An exemplary evaluation procedure and determination of the EEDF can be seen in Figure 3. We point out that this model assumes an isotropy of the plasma which is most likely not given. According to Lobbia et al.[19] an anisotropic effect on the electron current collection is mitigated when the anisotropic drifting beam component is parallel to the electrode surface. Furthermore it is stated in Lobbia et al.[19] that the effect of magnetic fields can be neglected in the limit of the probe radius being much smaller than the local Larmor radius, which is for our plasma most likely the case. Former studies regarding these contradictory recommendations (measuring parallel and orthogonal to the magnetic field lines, compare Figure 2) lead to the decision to measure in parallel orientation.[21] A strong anisotropy and non-Maxwellian behavior of the EEDF was observed for the MINOTOR prototype.[21] However, those measurements were carried out much closer to the thruster, about 6 cm.[21] Preliminary measurements regarding the relevance of the distance of the probe to the thruster allowed us to conclude that, at a greater distance, the orientation of the probe in relation to the magnetic field lines plays a negligible role. In addition, the non-Maxwellian character of the plasma could not be confirmed in that distance which was explained the smaller magnetic field strength in greater distance to the thruster.

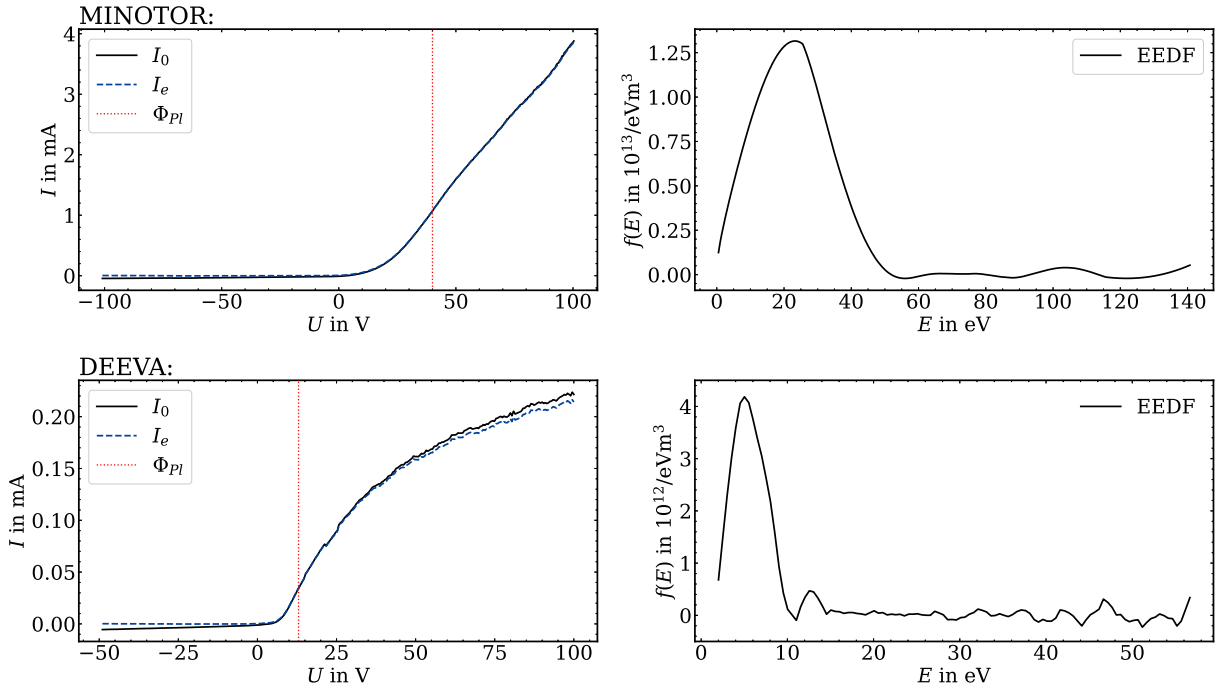

Figure 3. Exemplary evaluation of Langmuir probe data. The data of the MINOTOR prototype can be seen in the top row, at operation conditions 1 sccm of xenon, 30 W input power, and frequency set of 2450 MHz. The DEEVA thruster can be seen on the bottom, at 1 sccm of argon, 30 W input power, and frequency set of 2450 MHz. On the left the current-voltage characteristic I_0 can be seen. After subtracting the ion saturation current the resulting electron current I_e is depicted in blue. The vertical red line depicts the determined plasma potential Φ_{Pl}. In the MINOTOR case, the plasma potential is 42 V, in the DEEVA case it is 12 V. On the right, one can see the determined electron-energy distribution functions $f(E)$ respectively, showing in both thruster cases a single maxwellian character.

D. Retarding potential analyzer evaluation

A challenge arises when trying to extract information about the ion distribution function from a Langmuir probe, which operates at a positive potential, repelling ions, and draws electron-saturation current.[22] This electron saturation current is typically significant enough to overshadow any variations in the ion current that might provide insight into the ion temperature or energy distribution.[22] Therefore, more sophisticated analyzers, such as the "gridded energy analyzer", so called, retarding potential analyzers (RPAs) are often employed to obtain information about the ion energy distribution functions of plasmas. These devices consist of a system of grids at different potentials.[22] The operating principle is as follows: the first grid is kept electrically floating, allowing the measurement of a floating grid potential. In post-processing, this enables one to gain information about the actual energies measured. The second grid repels essentially all the electrons in the beam, allowing only ions to pass. The third grid is the ion retarding grid, where a positive potential U is sequentially set, allowing only ions exceeding the energy eU to pass and reach the collector.[22,23] The fourth grid, the secondary electron grid, suppresses electrons that may be produced by the ions hitting the collector.[22,23] It is possible to gain information about ion temperature and ion density with RPA measurements. An exemplary evaluation procedure can be seen in Figure 4. As one can see, the measured current value of the MINOTOR prototype exceeds the current of the plume of the DEEVA thruster by a factor of 10^6. This shows that there is much more current exiting the MINOTOR prototype than there is for the DEEVA thruster. However, since we cannot estimate the effect of additional charge densities existing between the grids (which can change the potential and therefore influence current measurements[22]), hence a quantitative determination of the ion density in the beam is not possible with this set up. Therefore, we focus on determining the maximum ion energy and ion energy distribution function (IEDF). The latter is determined by the first derivative of the measured current, the maximum of this distribution function is then the maximum ion energy $E_{\mathrm{i,max}}$. For both thrusters we determine a broadend, bi-maxwellian IEDF.

The RPA used is a commercial RPA from the company Plasma Controls, LLC. It has an entrance aperture of 12.7 mm and an overall transparency of 35 %. For the operation, picoamperemeters from Keithley with a resolution of 1 nA in the 2 mA range are employed.

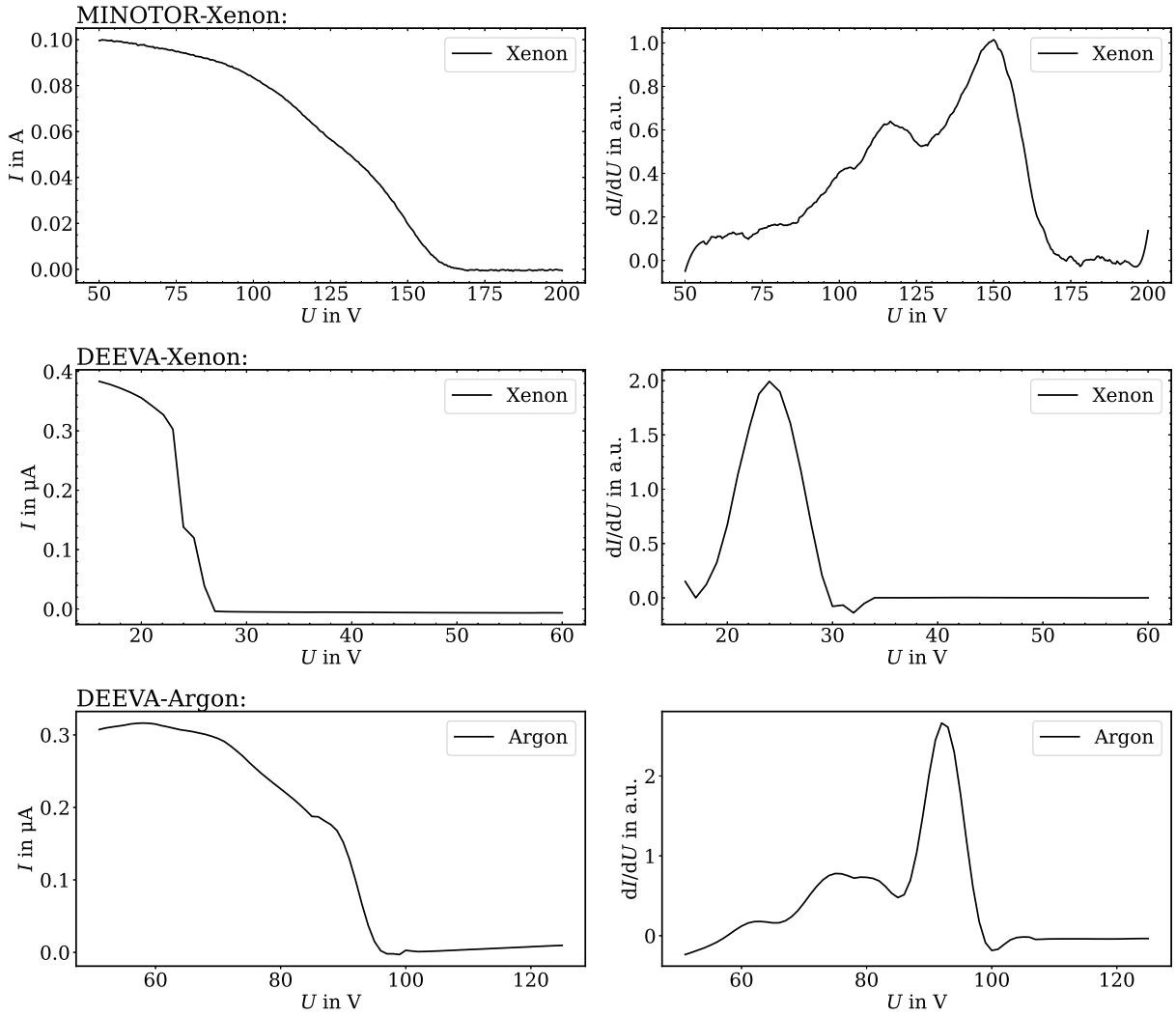

Figure 4. Exemplary evaluation of RPA data. The data of the MINOTOR prototype can be seen in the top row, at operation conditions 1 sccm of xenon, 30 W input power, and frequency set of 2450 MHz. The center row depicts the data of the operation of DEEVA with xenon as propellant at 1 sccm, 30 W input power, and frequency set of 2450 MHz. The operation of the DEEVA thruster with argon can be seen on the bottom row, at 1 sccm, 30 W input power, and frequency set of 2450 MHz. On the left the current-voltage characteristic of the RPA can be seen. On the right the first derivative of the raw current measurement $\mathrm{d}I/\mathrm{d}U$, the IEDF, can be seen. The maximum ion energy determined in this case for MINOTOR is approximately 150 eV, in the DEEVA case it is for xenon about 25 eV and for argon around 95 eV.

IV. Experimental results

As depicted in Figure 4 and Figure 5, the maximum ion energies determined for the DEEVA thruster are significantly higher when argon is used as the propellant instead of xenon. Despite identical thruster operational parameters — namely, same power, frequency, and volume flow rates — operation with argon yields multiple times higher maximum energies than operation with xenon. We measure ion energies up to 150 eV in case of operation with argon, while the operation with xenon leads to ion energies not exceeding 30 eV. Importantly, the magnetic field topology is the same in both cases. Furthermore, it can be noticed, that the

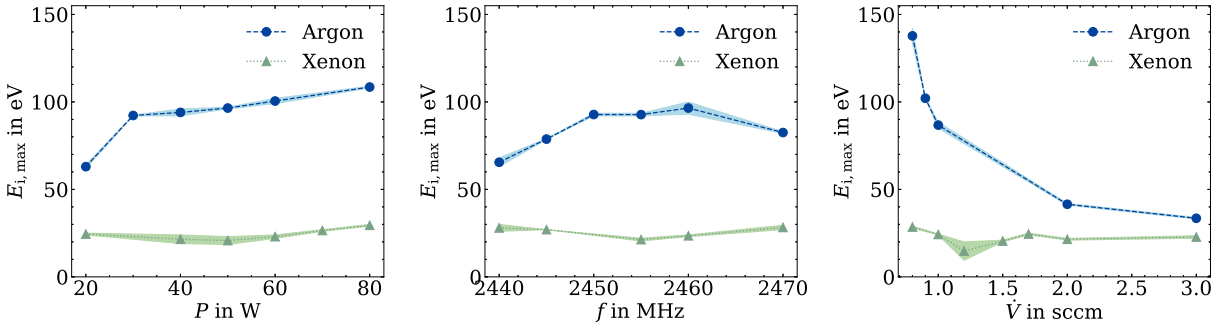

Figure 5. Maximum ion energies determined of the DEEVA thruster operated with xenon and argon as propellant. The plot on the left shows power variations at a frequency set of 2450 MHz and a volume flow of 1 sccm of argon (dashed line) and xenon (dash dotted line). The center plot depicts frequency variation at power input of 30 W and a volume flow of 1 sccm. The right hand side plot shows the volume flow variation at the constant frequency 2450 MHz and input power of 30 W. The error bars represent the standard deviation taken from multiple measurements.

electron temperature of the DEEVA thruster operated with xenon is not exceeding 2 eV over all parameter changes. Moreover, discernible trends can be observed from the parameter variations. In the left-hand plot of Figure 5, we see that the maximum ion energy also increases with increasing power at a frequency set to 2450 MHz and a volume flow of 1 sccm argon. For xenon, by comparison, the change in the determined ion energy seems to be negligible at the same power and volume flow setting. The same holds for the frequency variation at power input of 30 W and a volume flow of 1 sccm. While in case of argon a maximum ion energy can be detected at about the design frequency, the xenon curve seems to be independent of frequency variation. A clear decrease in ion energy can be seen with increasing volume flow of argon at constant frequency 2450 MHz and input power of 30 W, while in comparison the performance with xenon hardly changes.

As it is described before, the correlation of electron temperature and ion energy is a main driving force in a magnetic nozzle design. We can follow in the footsteps of previous research by comparing the trends and ratios of the two plasma parameter, electron temperature and maximum ion energy. A simple comparison of the trends can be seen in Figure 6. The left plot shows the electron temperate T_e and maximum ion energy $E_{i,max}$ determined in case of MINOTOR as a function of volume flow of xenon. With increased volume flow, the electron temperature, as well as the ion energy decreases. This is in accordance with observations reported in literature for the MINOTOR prototype, and can be explained by a decrease in free mean path length of the ions due to a higher neutral gas pressure. The same trends can be seen in the right plot for the DEEVA thruster operated at different volume flows of argon. Both thrusters are kept at 2450 MHz and input power of 30 W.

In Figure 7 the ratio of electron temperature and maximum ion energy E_i/T_e for variable thruster operational settings can be seen for the DEEVA and the MINOTOR prototype. The ratio for the MINOTOR prototype is plotted in blue and that for the DEEVA prototype in green. The plot on the left shows the dependence on power variations at a frequency set of 2450 MHz and a volume flow of 1 sccm of argon (in case of DEEVA) and xenon (in case of MINOTOR). The center plot depicts the dependence on frequency variation at power input of 30 W and a volume flow of 1 sccm. The right plot shows the dependence on volume propellant flow (of argon, in case of DEEVA; and xenon, in case of MINOTOR) at the constant frequency 2450 MHz and input power of 30 W. As one can see the resulting ratio in case of MINOTOR in blue is quite constant at a value of about 11 over all operational points. DEEVA in green shows a good correlation in dependence on power at a ratio of 19. However, in case of frequency and volume flow dependence, the correlation is not as constant as for MINOTOR case. Over all three operation parameter variations the ratio of electron temperature to maximum ion energy in case of MINOTOR is about 10 for xenon as propellant, while for DEEVA the ratio is in the range of 20 for argon as propellant.

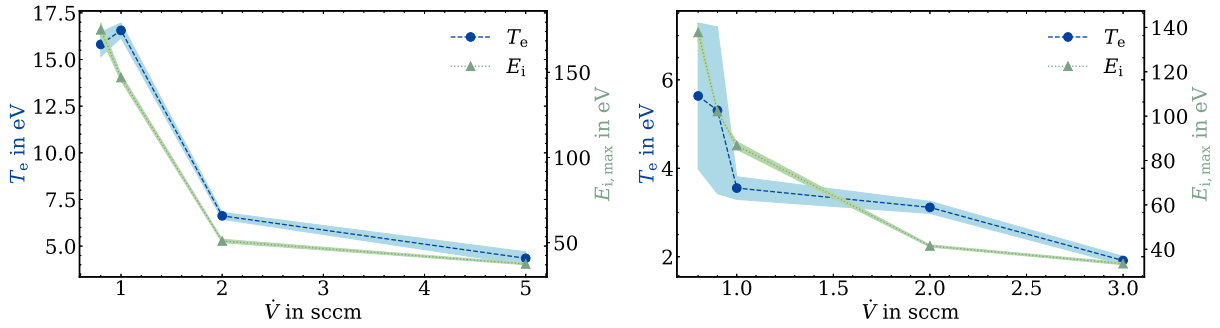

Figure 6. Correlation of electron temperature and maximum ion energy for MINOTOR on the left and DEEVA on the right at variable volume flow settings. MINOTOR is operated at 2450 MHz and input power of 30 W, the volume flow of xenon is varied. DEEVA on the right, is operated at 2450 MHz and input power of 30 W, and the volume flow of argon is varied. The electron temperature T_e can be seen in blue and its scale can be seen on the left. The maximum ion energy $E_{i,max}$ can be seen in green, with the scale on the right. The filled space shows the standard deviation of the resulting values from multiple measurements.

V. Conclusion

First and foremost, it is important to note that the LP and RPA are positioned in close proximity to the thruster. This proximity significantly influences the thruster's performance and the plasma parameters obtained. Despite the LP being oriented parallel to the magnetic field lines, which theoretically should enable the measurement of bi-Maxwellian shaped EEDFs, in most of the cases our observations reveal Maxwellian-shaped distribution functions for both thrusters, as shown in Figure 3. However, given our primary interest in electron temperature in this study, employing double Langmuir probe measurements could serve as an effective means to validate the results presented here.

Additionally, it is important to note that the testing chamber STG-MT is of medium size, which can potentially have a negative impact on the thruster's performance due to limitations in pumping speed. It is well established that higher background pressures result in a decrease in the mean free path lengths of plasma particles. Consequently, the decrease in ion energy and electron temperature observed for both the DEEVA and MINOTOR prototypes with increasing volume flow may be attributed to this phenomenon. Moreover, this could also contribute to the broadening of the ion energy distribution functions, as illustrated in Figure 4.

The significant disparity in electron temperature and ion energy observed during DEEVA operation with argon versus xenon, as shown in Figures 4 and 5, warrants further investigation. Currently, there is no conclusive theory to explain this phenomenon. We observe an overall better performance with argon as a propellant regarding electron temperature and maximum ion energy. These results have been reproduced on multiple occasions and seem to be a characteristic of the new DEEVA thruster. In contrast, literature indicates that MINOTOR prototypes exhibit different behavior when operated with argon. Specifically, the overall performance, including ion energy, ion current, specific impulse, and thrust, is not as good with argon as it is with xenon.[24] Since the setup and operational points remain unchanged when switching gases for our investigations on the DEEVA thruster, the only variable affecting thruster performance is the type of gas used. The observed differences can be therefore solely attributed to the differences in gas mass, the cross section for electron collisions, or/and ionization energy (15.76 eV for argon compared to 12.13 eV for xenon).

In existing literature, a constant ratio between electron temperature and maximum ion energy has often been observed. For instance, in the absence of a MN, a ratio of approximately 7 was reported, while stronger magnetic fields led to a ratio of 4.[10] We note a similar constant ratio in the case of the MINOTOR prototype, albeit with a ratio more than twice as high as previously reported values. This discrepancy can be attributed to higher electron temperatures reported in the literature, where measurements exceeding 20 eV were recorded alongside similar or smaller ion energies, as determined in our case.[10] Understanding the variance between the results of the ECR thruster prototype in literature and our observations is challenging.

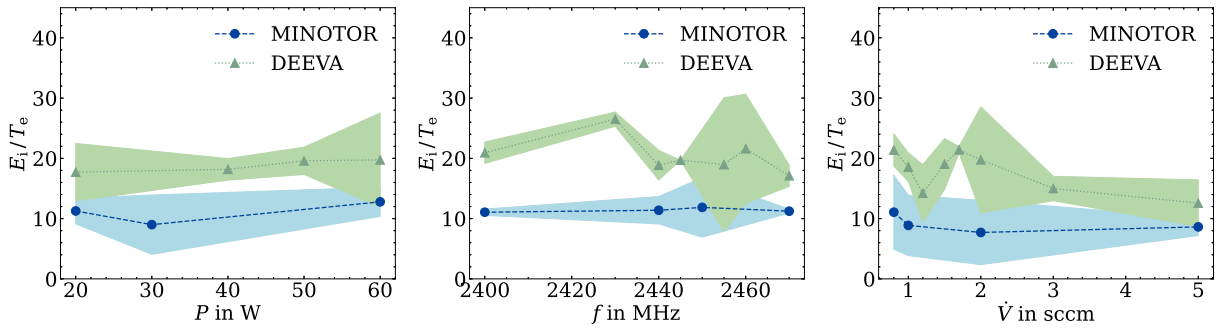

Figure 7. Ratio of electron temperature and maximum ion energy for variable thruster operational settings. The ratio of maximum ion energy and electron temperature E_i/T_e can be seen for both thrusters at variable input power, frequency and volume flow set. The MINOTOR prototype's ratio can be seen in blue, the DEEVA thruster's can be seen in green. The plot on the left shows power variations at a frequency set of 2450 MHz and a volume flow of 1 sccm of argon (in case of DEEVA) and xenon (in case of MINOTOR). The middle plot depicts frequency variation at power input of 30 W and a volume flow of 1 sccm. The right plot shows the volume flow variation (of again argon, in case of DEEVA; and xenon, in case of MINOTOR) at the constant frequency 2450 MHz and input power of 30 W. The filled space shows the standard deviation of the resulting values from multiple measurements.

Factors such as the thruster setup (including magnetic field and topology, microwave generator, cabling, and mass flow control unit), LP position, data acquisition and evaluation methods, ion energy detection method, and facility effects (e.g., chamber size, pumping rates); all play significant roles in determining plasma parameters and performance. This motivated our analysis on comparing the MINOTOR and DEEVA prototypes, both examined under identical conditions in the same vacuum chamber, with consistent background pressures, thruster setups, and diagnostic tools and methods. Our findings reveal a relatively constant ratio of electron temperature to ion energy in the MINOTOR case, suggesting that expansion is predominantly driven by electron dynamics, with higher electron temperatures resulting in higher ion energies. The DEEVA thruster operated with argon demonstrates a stable ratio in dependence on power variations and a relatively constant ratio of about 20 in case of frequency and volume flow variations. This can be attributed to comparable ion energies to MINOTOR (up to 150 eV) but significantly lower electron temperatures, not exceeding 12 eV. The extent to which these observed ratios are influenced by differences in magnetic field topologies, strengths, and microwave coupling mechanisms warrants the development of an analytical thruster model specific to the DEEVA thruster.

VI. Acknowledgment

Many thanks to the ONERA team for providing the MINOTOR prototype for the comparison measurements. Furthermore, warmest thanks to the ion thrusters research group at JLU for their tremendous effort and support during the preparatory measurement campaigns.

References

[1]J. Kim, K.-J. Chung, K. Takahashi, M. Merino, and E. Ahedo, "Kinetic electron cooling in magnetic nozzle: Experiments and modeling," *Plasma Sources Science and Technology*, 2022.

[2]M. Merino and E. Ahedo, "Magnetic nozzles for space plasma thrusters," *Encyclopedia of Plasma Technology*, vol. 2, pp. 1329–1351, 2017.

[3]J. Schmidt, J. Simon, and M. Grabe, "The deep thruster concept," *37th International Electric Propulsion Conference,Boston, USA*, 2022.

[4]T. Vialis, J. Jarrige, and D. Packan, "Geometry optimization and effect of gas propellant in an electron cyclotron resonance plasma thruster," in *Proc. 35th Int. Electr. Propuls. Conf*, pp. 1–12, 2017.

[5]D. Packan, P. Elias, J. Jarrige, T. Vialis, S. Correyero, S. Peterschmitt, J. Porto, M. Merino, A. Sánchez-Villar, E. Ahedo, *et al.*, "H2020 minotor: Magnetic nozzle electron cyclotron resonance thruster," in *36th International Electric Propulsion Conference*, 2019.

[6]S. Correyero, M. Merino, P.-Q. Elias, J. Jarrige, D. Packan, and E. Ahedo, "Characterization of diamagnetism inside an ecr thruster with a diamagnetic loop," *Physics of Plasmas*, vol. 26, no. 5, p. 053511, 2019.

[7]S. Correyero Plaza, J. Jarrige, D. Packan, and E. Ahedo Galilea, "Measurement of anisotropic plasma properties along the magnetic nozzle expansion of an electron cyclotron resonance thruster," in *35th International Electric Propulsion Conference (IEPC)*, 2017.

[8]S. Correyero, J. Jarrige, D. Packan, and E. Ahedo, "Plasma beam characterization along the magnetic nozzle of an ecr thruster," *Plasma Sources Science and Technology*, vol. 28, no. 9, p. 095004, 2019.

[9]D. Korzec, F. Werner, R. Winter, and J. Engemann, "Scaling of microwave slot antenna (slan): a concept for efficient plasma generation," *Plasma Sources Science and Technology*, vol. 5, no. 2, p. 216, 1996.

[10]T. Lafleur, F. Cannat, J. Jarrige, P. Elias, and D. Packan, "Electron dynamics and ion acceleration in expanding-plasma thrusters," *Plasma Sources Science and Technology*, vol. 24, no. 6, p. 065013, 2015.

[11]M. Merino and E. Ahedo, "Influence of electron and ion thermodynamics on the magnetic nozzle plasma expansion," *IEEE Transactions on Plasma Science*, vol. 43, no. 1, pp. 244–251, 2014.

[12]M. Martinez-Sanchez, J. Navarro-Cavallé, and E. Ahedo, "Electron cooling and finite potential drop in a magnetized plasma expansion," *Physics of Plasmas*, vol. 22, no. 5, 2015.

[13]D. Goebel and I. Katz, *Fundamentals of electric propulsion: ion and Hall thrusters*, vol. 1. John Wiley & Sons, 2008.

[14]U. Stroth, *Plasmaphysik*. Springer, 2011.

[15]A. Fridman and L. Kennedy, *Plasma physics and engineering*. CRC press, 2004.

[16]B. Longmier, E. Bering, M. Carter, L. Cassady, W. Chancery, F. C. Díaz, T. Glover, N. Hershkowitz, A. Ilin, G. McCaskill, *et al.*, "Ambipolar ion acceleration in an expanding magnetic nozzle," *Plasma Sources Science and Technology*, vol. 20, no. 1, p. 015007, 2011.

[17]M. Merino, J. Nuez, and E. Ahedo, "Fluid-kinetic model of a propulsive magnetic nozzle," *Plasma Sources Science and Technology*, vol. 30, no. 11, p. 115006, 2021.

[18]V. Demidov, S. Ratynskaia, and K. Rypdal, "Electric probes for plasmas: The link between theory and instrument," *Review of scientific instruments*, vol. 73, no. 10, pp. 3409–3439, 2002.

[19]R. Lobbia and B. Beal, "Recommended practice for use of langmuir probes in electric propulsion testing," *Journal of Propulsion and Power*, vol. 33, no. 3, pp. 566–581, 2017.

[20]M. Druyvesteyn, "Der niedervoltbogen," *Zeitschrift für Physik*, vol. 64, no. 11, pp. 781–798, 1930.

[21]C. Schäfer, J. Zorn, K. Holste, and P. Klar, "Influences on langmuir probe measurements by an ecr thruster with magnetic nozzle," *New Results in Numerical and Experimental Fluid Mechanics XIV*, 2023.

[22]I. Hutchinson, "Principles of plasma diagnostics," *Plasma Physics and Controlled Fusion*, vol. 44, no. 12, p. 2603, 2002.

[23]S. Lai and C. Miller, "Retarding potential analyzer: Principles, designs, and space applications," *AIP Advances*, vol. 10, no. 9, p. 095324, 2020.

[24]J. Jarrige, P.-Q. Elias, F. Cannat, and D. Packan, "Performance comparison of an ecr plasma thruster using argon and xenon as propellant gas," in *Proceedings of the 33rd International Electric Propulsion Conference*, pp. 2013–420, 2013.